

Mastering Agile Tasks with Limited Trials

Yihang Hu¹ Pingyue Sheng¹ Shengjie Wang^{1,2,3} Yang Gao^{1,2,3,†}

¹ Tsinghua University ² Shanghai Artificial Intelligence Laboratory

³ Shanghai Qi Zhi Institute [†] Corresponding author

Abstract: Embodied robots nowadays can already handle many real-world manipulation tasks. However, certain other real-world tasks (e.g., shooting a basketball into a hoop) are highly agile and require high execution precision, presenting additional challenges for methods primarily designed for quasi-static manipulation tasks. This leads to increased efforts in costly data collection, laborious reward design, or complex motion planning. Such tasks, however, are far less challenging for humans. Say a novice basketball player typically needs only ~ 10 attempts to make their first successful shot, by roughly imitating a motion prior and then iteratively adjusting their motion based on the past outcomes. Inspired by this human learning paradigm, we propose the Adaptive Diffusion Action Planning (ADAP) algorithm, a simple & scalable approach which iteratively refines its action plan by few real-world trials within a learned prior motion pattern, until reaching a specific goal. Experiments demonstrated that ADAP can learn and accomplish a wide range of goal-conditioned agile dynamic tasks with human-level precision and efficiency directly in real-world, such as throwing a basketball into the hoop in fewer than 10 trials. Project website: <https://adap-robotics.github.io/>.

Keywords: Agile dynamic tasks, Goal-conditioned action planning, Iterative action refinement

1 Introduction

In recent years, embodied robots have made significant progress in handling a wide range of real-world tasks [1, 2], largely driven by advancements in data-driven methods like reinforcement learning [3, 4] and imitation learning [5, 6]. Additionally, large vision-language-action models [2, 7, 8, 9] have expanded their capabilities, allowing robots to understand and perform more generalized tasks based on both visual perception and natural language instructions. However, despite these successes, certain real-world tasks, particularly those involving agile dynamic processes, remain challenging. One prominent example is shooting a basketball into a hoop. Unlike quasi-static tasks, dynamic tasks require high precision, agility, and real-time adaptability [10, 11]. Even small deviations of motion can lead to failures, making precise execution essential for success [12]. This creates unique challenges for existing approaches, which are often designed for quasi-static tasks and fail to account for the real-time agility and complex physical dynamics in non-quasi-static tasks.

Several common methods have been considered by researchers to address agile dynamic tasks. While these straightforward approaches have shown promise, they each come with limitations in dealing with real-world agile tasks. Sim2Real Transfer [11, 13] offers low-cost data collection, but suffers from domain gaps especially in dynamic tasks where simulators fail to capture the exact physical dynamics of the real world. Imitation learning [14, 15, 16] faces difficulties in obtaining high-quality expert data for dynamic tasks in real-world, as even human experts cannot guarantee a high success rate in tasks like basketball shooting, making expert demonstrations harder to obtain. Reinforcement learning [12, 13] requires large amounts of data that is both expensive and

time-consuming in real-world, and the design of reward functions introduces significant workload without generalizability. Analytical Motion Planning [17, 18] is the most traditional method that relies heavily on precise physical models, which are labor-intensive to design and difficult to scale for more complex dynamic tasks due to the intricacies of real-world dynamics.

Given the challenges of these existing methods, we approach the problem from a different perspective. Consider a real-world scenario: how does a novice basketball player, say a ten-year-old boy, make his first successful free throw? When stepping up to the line for the first time, he may rely on a basic motion pattern learned from observation or experience: perhaps mimicking an NBA player’s standard overhead shooting form or simply ungracefully tossing the ball forward. Regardless of the motion pattern, he can take his first shot and observe the trajectories and landing points of the ball as feedback, based on which he can adjust his actions for the next attempt (for instance, if the ball lands too short, he may increase force and motion amplitude by a certain amount). After a few iterations (say about 10 trials), he will likely make his first successful shot into the hoop.

Inspired by this learning paradigm, we introduce the **Adaptive Diffusion Action Planning (ADAP)** algorithm, a simple but effective method that could learn and solve such agile dynamic tasks with excellent performance and efficiency. ADAP highlights the following two features:

- **Conditional Action Planning:** ADAP uses a *Conditional Action Planner* with diffusion backbone [19] to learn and model the common motion pattern of the few provided prior demonstrations. This planner can generate new actions within the same pattern, with respect to new conditioned set for new goals.
- **Iterative Action Plan Refinement:** Following the human learning paradigm stated above, ADAP iteratively rolls out the newly generated action plans and adaptively alters them using a *Condition Adapter* with Bayesian optimization backbone [20, 21], based on rough perception of the rollout results.

Our primary contribution is formalizing a common type of agile dynamic tasks and proposing the **Adaptive Diffusion Action Planning** algorithm. We verified its excellent performance and efficiency on these tasks in both simulator and real-world (e.g. It can throw a basketball into an arbitrarily located hoop in fewer than 10 trials). We further demonstrate that the self-correction paradigm of ADAP naturally enables generalization to similar tasks. Please refer to the later sections for details.

2 Tasks Setup

Our ADAP algorithm is designed for a general kind of agile dynamic tasks that appear commonly in real-world scenarios. To help better understanding the detailed process and application scenarios of ADAP, we give a brief introduction of specific task setups in this section before depicting the detailed algorithm later in Section 3.

We build three specific real-world agile dynamic tasks to be accomplished for experiments in our laboratory, listed as follows: (Layouts are shown in Figure 1.)

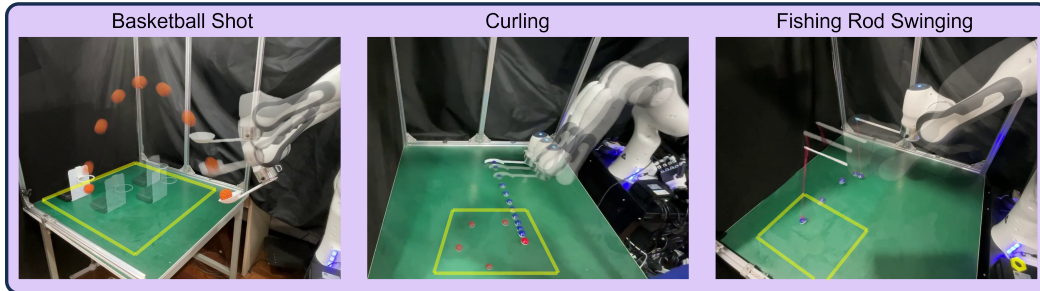


Figure 1: Overview of task layouts & processes. The table is an about 1 meter sized square and the yellow area indicates the rough range of reachable goals (e.g. where can the hoop be placed).

1. **Basketball Shot:** The robot arm is expected to throw a toy basketball into a hoop located arbitrarily on the table, with a spoon-shaped end effector which allows the toy ball to detach naturally from the end effector through smooth acceleration changes. This is consistent with how human make these shots.
2. **Curling:** The robotic arm uses a bar-shaped end effector to push the curling stone from a fixed starting point to a certain speed, and then let it slide while decelerating naturally on the table surface. The goal is to let it stop at a precise position just in front of a target stone.
3. **Fishing Rod Swinging:** The robotic arm equipped with a rod-like end effector attempts to cast the ‘hook’ swiftly onto the target location on the table by swinging the rod. The ‘hook’ is connected to the rod with a soft rope, which challenges the control of its position.

These three tasks are carefully selected to cover several typical agile dynamic behaviors that are commonly seen in daily life, including projectile motion, sliding with friction, and movement of soft deformable objects. They share some common properties as follows: **1.** These tasks involve short horizon agile dynamic processes whose results depend sensitively on a complete motion. **2.** Motions that can reach goals stably are usually smooth and time-consecutive. **3.** The difficulty of these tasks aligns with that of the daily tasks encountered by humans, where they can achieve favorable outcomes through a few number (~ 10) of trials and practice. **4.** These tasks are directly built in real-world with no reliance on simulators.

3 Method

3.1 Problem Formulation

We first present our formulation of this general kind of daily agile dynamic tasks, by first giving some basic analysis of task properties and the related assumptions we made with respect to the human learning paradigm, and then presenting the mathematical formulations.

3.1.1 Basic Assumptions

Real-world agile dynamic tasks typically involve rapid execution of continuous actions, which function together to trigger a specific non-quasi-static process and ultimately achieve a designated goal. It is hard even for humans to adjust the motion online based on real-time feedback in such swift process. However, humans are still able to efficiently complete such tasks through a rough imitation of a prior motion pattern and some minimal trial-and-error attempts. We abstract such task properties and the human learning paradigm into the following assumptions.

Open-loop Planning: For a lot of agile dynamic tasks in human daily life, the actual effective execution time of its dynamic process is usually short (e.g. a basketball player finishes the shooting motion in less than 1 second). So the closed-loop MDP setting commonly used for quasi-static manipulation tasks is less appropriate in these situations, due to the sensitive physical dynamics and the ineluctable latencies in perception & reaction. So we naturally adopt the open-loop planning setting, in which we always let the robot execute complete action plans (consisting of frame-level actions across all timesteps) without any reliance on intermediate perceptions. This resembles how humans perform such tasks: Design the entire motion in mind and execute it completely without interruption.

Prior Motion Pattern: One key component of the human learning paradigm is the knowledge of an initial prior of a specific motion pattern (e.g. the standard overhead shooting posture of an NBA player), which is capable to reach goals within a certain range of the environment. As humans can learn such rough prior motion pattern from very few demonstrations, we similarly assume a small dataset of prior action plans (which may come from any data collection method) to be available for the agent in each of the tasks we designed, to enable learning of an inherent motion pattern.

Rough Error Feedback: For daily dynamic processes, humans try to reach goals by refining their motions during iterative trials, based on some rough feedback they observe. (e.g. A basketball

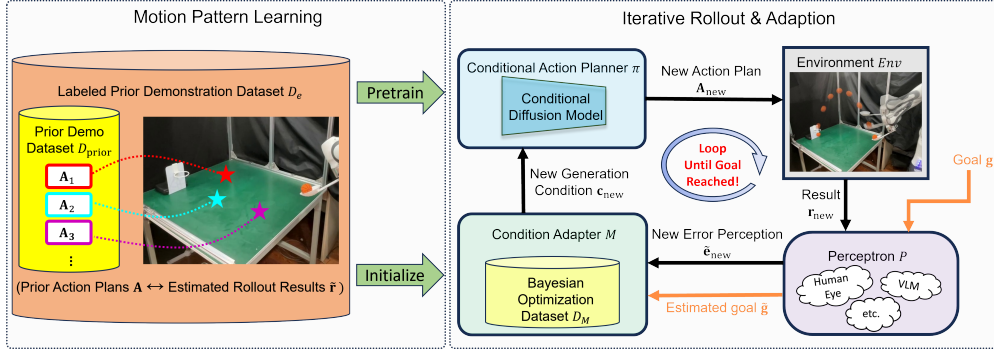


Figure 2: Overview of Adaptive Diffusion Action Planning (ADAP) with its two stages: Motion Pattern Learning (left) and Iterative Rollout & Adaption (right). The perceptron P might be human eye in our experiments or be replaced by VLM in future works (more discussions in Appendix A.1).

player sees that their last shot is short for about 30 cm, and is about 20 cm aside to the left. This forms a 2d vector as a rough feedback that instructs the player to adjust the motion for the next shot, by shooting a little to the right side and add some force.) We inherit the similar setting from such human learning paradigm, by allowing the agent to access a rough estimate of low-dim vectorized error after each rollout on a task as feedback. This inaccurate error estimation is enough to provide a rough optimization direction for the next attempts.

3.1.2 Mathematical Formulation

We present the mathematical formulation based on the assumptions mentioned before. A specific agile dynamic task environment (denoted by Env) would take an action plan $\mathbf{A} = \{\mathbf{a}_t \mid t \in [H]\}$ as input and then output a vectorized result \mathbf{r} as follows:

$$\mathbf{r} = rollout(\mathbf{A}), \mathbf{r} \in \mathbb{R}^k, \quad (1)$$

where \mathbf{a}_t is a frame-level robot action at timestep t , H stands for the horizon length (number of timesteps) and k stands for the dimensionality of the result space.

For the rollout result \mathbf{r} , we only need to observe a rough difference between \mathbf{r} and a desired goal \mathbf{g} (as claimed in Section 3.1.1), denoted by

$$\tilde{\mathbf{e}} = P(\mathbf{e}); \quad \mathbf{e} = \mathbf{r} - \mathbf{g}; \quad \tilde{\mathbf{e}}, \mathbf{e} \in \mathbb{R}^k \quad (2)$$

where \mathbf{e} stands for the ground-truth vectorized error and $\tilde{\mathbf{e}}$ stands for the estimate that we can observe, by a rough perceptron P . More detailed and clearer explanations about this perceptron P are provided in Appendix A.1.

The purpose of our algorithm is to produce some final action plan \mathbf{A}_f that accomplishes a new goal \mathbf{g} within a minimal number of real-world trials:

$$\mathbf{A}_f = Algorithm(Env, D_{prior}, \mathbf{g}) \quad \text{s.t.} \quad \tilde{\mathbf{e}} = P(rollout(\mathbf{A}_f) - \mathbf{g}) \approx \mathbf{0}, \quad (3)$$

where $D_{prior} = \{\mathbf{A}_i\}$ is a given dataset containing very few action plans (6-8 throughout our experiments) within the same motion pattern, as prior demonstrations.

3.2 Main Algorithm

ADAP aims to emulate the human learning paradigm to generate an action plan that successfully reaches a specified goal with few real-world interactions. It can be divided into the following two stages: **Motion Pattern Learning** and **Iterative Rollout & Adaption**. See an overview of the main pipeline in Figure 2 and pseudocode in Algorithm 1.

3.2.1 Motion Pattern Learning

Humans can approach the goal closer and closer by iterative trials, but a prerequisite is that they know a prior motion pattern and a rough correlation between the motion change and the result

change. So in this first stage, we try to endow our agent with knowledge of the prior motion pattern, along with a rough mapping between the rollout result \mathbf{r} and the corresponding action plan \mathbf{A} . We start by rolling-out all action priors in D_{prior} , and record the rough estimates of the rollout results with respect to $\mathbf{g}_0 = \mathbf{0}$:

$$D_e = \{(\mathbf{A}_i, \tilde{\mathbf{r}}_i) \mid \tilde{\mathbf{r}}_i = P(\text{rollout}(\mathbf{A}_i) - \mathbf{g}_0), \mathbf{A}_i \in D_{\text{prior}}, \mathbf{g}_0 = \mathbf{0}\} \quad (4)$$

With this initial labeled dataset D_e , we set a *Conditional Action Planner* $\pi : \tilde{\mathbf{r}} \rightarrow \mathbf{A}$ for mapping a rough rollout outcome back to the action plan. We adopt a U-Net based diffusion model for π and train it with D_e by the diffusion model loss function [19].

3.2.2 Iterative Rollout & Adaption

For an unseen goal \mathbf{g} estimated as $\tilde{\mathbf{g}} = P(\mathbf{g})$, the action plan $\mathbf{A}_c = \pi(\tilde{\mathbf{g}})$ can hardly reach the goal directly by the first trial, because the training set D_e contain very few samples that cannot cover the entire goal space, and all goal estimations from prior results contain errors. However, the motion pattern is already learned by π . So by treating the input goal of π as a generation condition, we can do effective exploration within the learned motion pattern through searching for the best generation condition. Besides, the rough error feedback $\tilde{\mathbf{e}}$ can provide a rough direction for this optimization process, this is just like how human refine their motions.

Specifically, we freeze the trained π , and use \mathbf{c} instead of $\tilde{\mathbf{g}}$ to denote the generation condition of π . Then with a given \mathbf{g} , the perception result of an action plan generated by π can be written as a function of the generation condition \mathbf{c} :

$$\tilde{\mathbf{e}}(\mathbf{c}) = P(\text{rollout}(\mathbf{A}_c) - \mathbf{g}) = P(\text{rollout}(\pi(\mathbf{c})) - \mathbf{g}). \quad (5)$$

And our purpose turns to be optimizing for the best \mathbf{c} until $\tilde{\mathbf{e}}(\mathbf{c})$ is close enough to zero:

$$\mathbf{c}^{\text{optimal}} = \arg \min_{\mathbf{c}} \|\tilde{\mathbf{e}}_{\mathbf{g}}(\mathbf{c})\| \quad (6)$$

We adopt a GPR-based Bayesian optimization model (denoted as $M : \mathbf{g} \rightarrow \mathbf{c}$) to serve as a *Condition Adapter*, which hopefully maps an observed goal $\tilde{\mathbf{g}}$ back to the correct generation condition \mathbf{c} . This module is built upon dataset $D_M = \{(\mathbf{c}, \tilde{\mathbf{g}})\}$, which is initially filled by data from D_e :

$$D_M = \{(\mathbf{c}_i, \tilde{\mathbf{g}}_i) \mid \mathbf{c}_i = \tilde{\mathbf{g}}_i = \tilde{\mathbf{r}}_i, (\mathbf{A}_i, \tilde{\mathbf{r}}_i) \in D_e\}. \quad (7)$$

We generate $\mathbf{c}^{\text{new}} = M(\tilde{\mathbf{g}})$ and observe $\tilde{\mathbf{e}}^{\text{new}} = \tilde{\mathbf{e}}(\mathbf{c}^{\text{new}})$ by Equation 5. Then we append a new data pair $(\mathbf{c}^{\text{new}}, \tilde{\mathbf{g}}^{\text{new}})$ into D_M , where

$$\tilde{\mathbf{g}}^{\text{new}} = \tilde{\mathbf{g}} + \tilde{\mathbf{e}}^{\text{new}}. \quad (8)$$

This updated D_M would contain more information that helps the *condition adapter* M to propose a better generation condition \mathbf{c}^{new} for the next trial, with respect to the same desired goal $\tilde{\mathbf{g}}$. By iterating this rollout-updating process, the error $\tilde{\mathbf{e}}$ would converge to zero quickly, so that the goal is reached successfully in very few rounds, just like the few attempts humans make before accomplishing a new task.

3.3 Other Techniques

Timeline Shifting Augmentation. Our prior dataset D_{prior} contains only as few as ~ 10 demonstrations, so that π is likely to overfit by memorizing frame-actions at specific timesteps, and this is harmful to its learning of the inherent motion pattern. We use the *Timeline Shifting Augmentation* technique to augment the training dataset D_e of π . Specifically, a specific action plan is augmented by randomly cutting off a small fragment at the start or end of its time horizon, and padding the other side with the nearest frame-action to make the horizon length H consistent with the original action plan. This multiplies the total amount of training data, and helps π focus more on learning the complete motion structure, rather than overfitting to specific timesteps. Detailed definitions of this technique are presented in Appendix A.2.

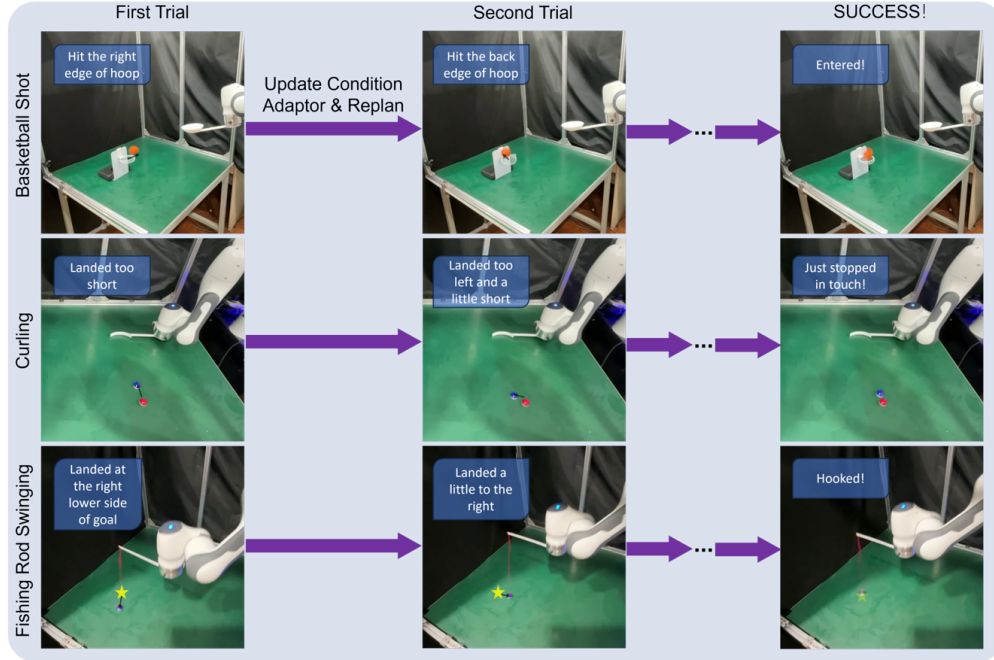


Figure 3: **Iterative Rollout & Adaption** process of ADAP on the three real-world tasks. The small black errors indicates the vectorized error to be estimated. The yellow star for the *Fishing Rod Swinging* task indicates the goal, which is too small to be obviously seen.

Data Forgetting. The current *Condition Adapter* with the GPR-Bayesian optimization backbone tends to memorize all past trials in D_M to give the best generation condition proposal for the next trial. For most cases it successfully find the proper condition in very few iterations, but occasionally some dirty data might occur, either because the environment suffer some unknown disturbance, or because the perceptron P happens to produce a too inaccurate error estimation. If such dirty data are appended into D_M , this adapter may get stuck and fail to find a successful condition. We resolve this issue by retaining only the latest 2 trials in D_M during stage 2, (the initial data pairs from stage 1 are always kept), so that even if some dirty data are appended to D_M by chance, it is forgotten in 2 rounds and our algorithm can still reach the goal quickly afterwards.

4 Experiments & Evaluations

4.1 Main Experiments in Real-world

Task Scenes: We apply ADAP to the three real-world agile dynamic tasks introduced in Section 2. The construction of all these tasks are inspired from daily scenes, and are in accordance with our assumptions made in Section 3.1.1. These tasks are

Task	Prior Demo Source	Frame Action Format
<i>Basketball Shot</i>	Simulator	Joint pose
<i>Curling</i>	Tele-operation	Joint pose
<i>Fishing Rod Swinging</i>	Tele-operation	End-effector pose

Table 1: Settings of prior demonstration dataset D_{prior} for our tasks. The format of action plans generated later are always in accordance with the corresponding priors.

performed by a Franka Emika Panda robot arm with specially designed end effectors respectively (Figure 5). For all three tasks, the goals are arbitrarily set on the 2D table surface by concrete objects (e.g. the basketball hoop, or the curling stone to be hit) within a reachable range of the corresponding tasks, and any rollout requires very high precision to be judged as a success. Some settings about the prior dataset D_{prior} that vary along the three tasks are listed in Table 1. Besides, to verify the generalizability of ADAP across similar tasks, we built two modified versions of the tasks *Basketball Shot-V2* and *Basketball Shot-V3*. These two modified versions involve different hardware, but

Task	Prior Demo Num (Stage1)	Avg Num of Adapt Trials (Stage2)	Total Num of Trials
<i>Basketball Shot</i>	6	3.0 ± 0.5	9.0
<i>Curling</i>	6	3.4 ± 1.1	9.4
<i>Fishing Rod Swinging</i>	8	2.0 ± 0.4	10.0
<i>Basketball Shot-V2</i>	6	3.1 ± 0.6	9.1
<i>Basketball Shot-V3</i>	6	3.8 ± 1.2	9.8

Table 2: Main evaluation results in real-world tasks. Fewer number of trials indicates better performance. The bottom 2 tasks are modified versions of the original *Basketball Shot* task, with changed hardware conditions, as showed in Figure 5.

directly share the same prior demo dataset of the original version. Due to limited pages, please refer to Appendix B for the full details of these real-world task scene setups.

Evaluation Metric: The main motivation of ADAP is to mimic the human learning paradigm so that it reaches a goal precisely with minimal number of real-world trials. So the main metric throughout our experiments is the number of trials (denoted by N) performed until the firstly reaching the goal g . Note that in the same task scene, when the goal changes to a new position, the first stage of the algorithm does not need to be run again. We count the total number of trials (N) as the number of prior rollouts ($|D_{\text{prior}}|$) in stage 1 plus the average number of trials in stage 2. This sum indicates how many trials are required to reach the FIRST unseen goal.

Real-world Experimental Results: For all three tasks we do 2 groups of experiments, each with different prior demonstration sets, and we set 5 goals to be reached in each group. To make our presented results reliable and convincing, these goals are deliberately set not to be achievable directly by the prior demonstrations. Result statistics are shown in Table 2.

We see that although all three tasks require high precision to be judged as success, they each require only about 10 trials in expectation to reach their first goals successfully. And for secondary new goals, as few as about 3 more trials are enough. This is somehow consistent with the fact that humans can reach the second goal much faster than the first one, as they have become more experienced on that specific task and the corresponding motion pattern.

Consider the *Basketball Shot* task (referred to as *V1* for short), its two modified versions (*V2* & *V3* for short) in real-world involve different hardware parameters respectively, and these modifications of physical conditions can lead to obviously changed rollout results, given the same action plan. However, although the prior demonstrations provided to *V2* and *V3* are generated by the simulator aligned to *V1*, they suffer little performance drop as shown in Table 2. This proves that the motion pattern learned from the prior demos can indeed be used to solve a generalized range of similar tasks, rather than being limited to scenarios with specific physical parameters.

4.2 Comparisons & Ablations

We use the simulator built for *Basketball Shot* to enable and comparisons between ADAP and 2 baselines based on motion planning: **Interpolation of Nearest Neighbors** directly interpolates the action plans in D_e by weights computed from goal estimations; **Interpolation of Nearest Neighbors Aligned** is the same method with the prior demonstrations carefully aligned along the timeline. See detailed definitions in Appendix C.2. Besides, we also do ablation studies to assess the 2 techniques introduced in Section 3.3: **ADAP w/o Timeline Shifting Augmentation** and **ADAP w/o**

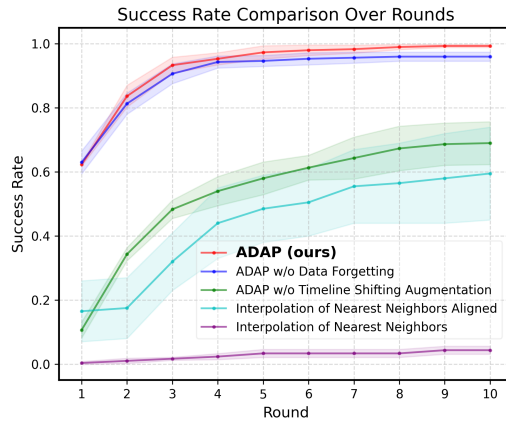


Figure 4: Success rates of ADAP and baselines across different rounds, on task *Basketball Shot* in simulator.

Data Forgetting. We evaluate the performance of these baselines by success rate along different rounds (e.g. value 0.8 in round 2 means that 80% of goals are reached in ≤ 2 trials), as the number of trials for a specific goal might go to infinity. Results are plotted in Figure 4. We can see that ADAP achieves high performance consistent with real-world experiments, while each of the other baselines suffers some performance drop. As for the ablations, *Timeline Shifting Augmentation* increase the performance a lot by letting π focus on learning the motion while avoiding overfitting; *Data Forgetting* provides small increment on the converged success rate by dropping the possibly dirty data that limits the condition adaption quality. More details are in Appendix C.3.

5 Related Works

Agile Dynamic Task Performing. Achieving agile and dynamic task performance in robotics has been explored through various approaches. Recent works [22, 23, 24] have demonstrated significant progress in achieving agile locomotion and dynamic tasks for quadrupedal robots. Beyond locomotion, works like [25, 12, 10, 26, 27, 11] adopt data-driven methodologies to enhance control commands by leveraging partial dynamic models for optimization. While these approaches have demonstrated impressive capabilities, they often demand large amounts of training data, requiring millions of interaction samples and sophisticated simulation environments. In contrast, our work leverages imitation learning techniques to enable comparable or superior performance with orders of magnitude less data, eliminating the need for reward engineering and addressing the complex simulator design while maintaining high performance standards for agile dynamic tasks, thus making these advanced robotic capabilities more accessible and practical for real-world applications.

Goal-conditioned Policy Learning. Goal-conditioned policy learning has gained significant attention in the field of robotics due to its ability to enable robots to autonomously perform tasks based on specific goals. Goal-conditioned reinforcement learning (GCRL) has been studied in a number of prior works [28, 29, 30, 31, 26, 32, 33, 34, 35]. Apart from GCRL, recent works [36, 37, 38, 39, 40, 12, 38] offer an alternative approach to solving this problem in a more data-efficient manner using imitation learning (IL). Our method differs from previous approaches in that we explicitly design the diffusion process to handle the high temporal precision required for agile tasks. This design allows our system to maintain high performance in dynamically challenging environments with as few as 10 demonstration trajectories.

Learning from Feedback. The integration of data-driven and analytical models has proven highly effective for robotic action execution. A dominant paradigm focuses on learning residual policies that systematically compensate for the discrepancies of a nominal behavior policy [41, 42, 43, 44, 45, 46, 47], while another line of work combines learned modules with classical physical-dynamics models to rectify errors in analytical approximations [48, 49, 12]. Iterative refinement has been applied to tasks such as assembly and precision manipulation, with success in overcoming model inaccuracies. Unlike these approaches, our method uniquely implements target position refinement for agile tasks. Our approach eliminates the need for complex reward engineering or large datasets, offering an intuitive solution that naturally transfers across different robotic arms and physical conditions while effectively compensating for systematic errors in arm dynamics.

6 Conclusion

In this paper, we formalize and study a general kind of goal-conditioned agile dynamic tasks commonly seen in real-world. We introduce the Adaptive Diffusion Action Planning algorithm, which draws inspiration from human learning paradigms. Our experiments have shown that ADAP is able to learn and solve such agile dynamic tasks directly in real-world, with excellent data efficiency and performance comparable to humans. Besides, the naturally emerged generalizability of ADAP enables wide application to similar task scenes. We hope that this work provides a new inspiring insight into letting embodied agents learn and solve more generalized real-world tasks efficiently.

7 Limitations

Despite the achievements claimed above, we can still see some significant limitations of this work: For example, this algorithm rely heavily on high-quality prior demonstrations, meaning that the inherent motion pattern need to concentrate, but the result spreading should diverse. Another limitation is that, our method could only be applied to the tasks with clearly defined vectorized error feedback that changes smoothly with respect to action changes. A counterexample is the *Basketball Shot* task with bouncing process: If we allow the ball to bounce for any times on the floor or with obstacles before entering the hoop, then ADAP would fail since the intermediate dynamic process is multi-modal and chaotic, and is unable to provide well-defined vectorized feedback. We hope that future researchers can resolve these issues and delve deeper into this research area, to expand the capabilities of embodied agents and bringing them one step closer to human-level intelligence.

References

- [1] T. He, J. Gao, W. Xiao, Y. Zhang, Z. Wang, J. Wang, Z. Luo, G. He, N. Sobanbab, C. Pan, Z. Yi, G. Qu, K. Kitani, J. Hodgins, L. J. Fan, Y. Zhu, C. Liu, and G. Shi. Asap: Aligning simulation and real-world physics for learning agile humanoid whole-body skills. *Robotics: Science and Systems*, 2025.
- [2] K. Black, N. Brown, D. Driess, A. Esmail, M. Equi, C. Finn, N. Fusai, L. Groom, K. Hausman, B. Ichter, S. Jakubczak, T. Jones, L. Ke, S. Levine, A. Li-Bell, M. Mothukuri, S. Nair, K. Pertsch, L. X. Shi, J. Tanner, Q. Vuong, A. Walling, H. Wang, and U. Zhilinsky. π_0 : A vision-language-action flow model for general robot control. *arXiv preprint arXiv:2410.24164*, 2024.
- [3] Y. Zhang, T. Liang, Z. Chen, Y. Ze, and H. Xu. Catch it! learning to catch in flight with mobile dexterous hands. *IEEE International Conference on Robotics and Automation*, 2024.
- [4] W. Ye, Y. Zhang, H. Weng, X. Gu, S. Wang, T. Zhang, M. Wang, P. Abbeel, and Y. Gao. Reinforcement learning with foundation priors: Let the embodied agent efficiently learn on its own. *arXiv preprint arXiv:2310.02635*, 2023.
- [5] H. Bharadhwaj, J. Vakil, M. Sharma, A. Gupta, S. Tulsiani, and V. Kumar. Roboagent: Generalization and efficiency in robot manipulation via semantic augmentations and action chunking. *IEEE International Conference on Robotics and Automation*, 2023. doi: [10.1109/ICRA57147.2024.10611293](https://doi.org/10.1109/ICRA57147.2024.10611293).
- [6] H. Ha, Y. Gao, Z. Fu, J. Tan, and S. Song. UMI on legs: Making manipulation policies mobile with manipulation-centric whole-body controllers. In *Proceedings of the 2024 Conference on Robot Learning*, 2024.
- [7] A. Brohan, N. Brown, J. Carbajal, Y. Chebotar, J. Dabis, C. Finn, K. Gopalakrishnan, K. Hausman, A. Herzog, J. Hsu, J. Ibarz, B. Ichter, A. Irpan, T. Jackson, S. Jesmonth, N. J. Joshi, R. Julian, D. Kalashnikov, Y. Kuang, I. Leal, K.-H. Lee, S. Levine, Y. Lu, U. Malla, D. Manjunath, I. Mordatch, O. Nachum, C. Parada, J. Peralta, E. Perez, K. Pertsch, J. Quiambao, K. Rao, M. Ryoo, G. Salazar, P. Sanketi, K. Sayed, J. Singh, S. Sontakke, A. Stone, C. Tan, H. Tran, V. Vanhoucke, S. Vega, Q. Vuong, F. Xia, T. Xiao, P. Xu, S. Xu, T. Yu, and B. Zitkovich. Rt-1: Robotics transformer for real-world control at scale. *Robotics: Science and Systems*, 2022.
- [8] M. J. Kim, K. Pertsch, S. Karamcheti, T. Xiao, A. Balakrishna, S. Nair, R. Rafailov, E. Foster, G. Lam, P. R. Sanketi, Q. Vuong, T. Kollar, B. Burchfiel, R. Tedrake, D. Sadigh, S. Levine, P. Liang, and C. Finn. Openvla: An open-source vision-language-action model. *Conference on Robot Learning*, 2024. doi:[10.48550/arXiv.2406.09246](https://doi.org/10.48550/arXiv.2406.09246).
- [9] S. Liu, L. Wu, B. Li, H. Tan, H. Chen, Z. Wang, K. Xu, H. Su, and J. Zhu. Rdt-1b: a diffusion foundation model for bimanual manipulation. *arXiv preprint arXiv: 2410.07864*, 2024.

- [10] C. Chi, B. Burchfiel, E. Cousineau, S. Feng, and S. Song. Iterative residual policy: for goal-conditioned dynamic manipulation of deformable objects. *The International Journal of Robotics Research*, 43(4):389–404, 2024.
- [11] B. Huang, Y. Chen, T. Wang, Y. Qin, Y. Yang, N. Atanasov, and X. Wang. Dynamic handover: Throw and catch with bimanual hands. *Conference on Robot Learning*, 2023. doi:10.48550/arXiv.2309.05655.
- [12] A. Zeng, S. Song, J. Lee, A. Rodriguez, and T. Funkhouser. Tossingbot: Learning to throw arbitrary objects with residual physics. *IEEE Transactions on Robotics*, 36(4):1307–1319, 2020.
- [13] H. Munn, B. Tidd, D. Howard, and M. Gallagher. Whole-body dynamic throwing with legged manipulators. *arXiv preprint arXiv:2410.05681*, 2024.
- [14] X. B. Peng, E. Coumans, T. Zhang, T.-W. Lee, J. Tan, and S. Levine. Learning agile robotic locomotion skills by imitating animals. *Robotics: Science and Systems*, 2020.
- [15] H. Chen, C. Zhu, Y. Li, and K. Driggs-Campbell. Tool-as-interface: Learning robot policies from human tool usage through imitation learning. *arXiv preprint arXiv:2504.04612*, 2025.
- [16] B. Xu, M. U. Din, and I. Hussain. Conditional variational auto encoder based dynamic motion for multi-task imitation learning. *arXiv preprint arXiv: 2405.15266*, 2024.
- [17] A. Sintov and A. Shapiro. A stochastic dynamic motion planning algorithm for object-throwing. In *2015 IEEE International Conference on Robotics and Automation (ICRA)*, pages 2475–2480. IEEE, 2015.
- [18] O. Taylor and A. Rodriguez. Optimal shape and motion planning for dynamic planar manipulation. *Autonomous Robots*, 43:327–344, 2019.
- [19] C. Chi, Z. Xu, S. Feng, E. Cousineau, Y. Du, B. Burchfiel, R. Tedrake, and S. Song. Diffusion policy: Visuomotor policy learning via action diffusion. *The International Journal of Robotics Research*, page 02783649241273668, 2023.
- [20] J. Mockus, V. Tiesis, and A. Zilinskas. *The application of Bayesian methods for seeking the extremum*, volume 2, pages 117–129. 09 2014. ISBN 0-444-85171-2.
- [21] C. Rasmussen, O. Bousquet, U. Luxburg, and G. Rätsch. Gaussian processes in machine learning. *Advanced Lectures on Machine Learning: ML Summer Schools 2003, Canberra, Australia, February 2 - 14, 2003, Tübingen, Germany, August 4 - 16, 2003, Revised Lectures*, 63-71 (2004), 3176, 09 2004. doi:10.1007/978-3-540-28650-9_4.
- [22] J. Hwangbo, J. Lee, A. Dosovitskiy, D. Bellicoso, V. Tsounis, V. Koltun, and M. Hutter. Learning agile and dynamic motor skills for legged robots. *sci. Robotics*, 4:26, 2019.
- [23] T. He, C. Zhang, W. Xiao, G. He, C. Liu, and G. Shi. Agile but safe: Learning collision-free high-speed legged locomotion. In *Robotics: Science and Systems (RSS)*, 2024.
- [24] L. Han, Q. Zhu, J. S. na, C. Z. na, T. L. na, Y. Zhang, H. Z. na, Y. Liu, C. Zhou, R. Zhao, J. Li, Y. Zhang, R. Wang, W. Chi, X. Li, Y. Zhu, L. Xiang, X. Teng, and Z. Zhang. Lifelike agility and play in quadrupedal robots using reinforcement learning and generative pre-trained models. *Nature Machine Intelligence*, 2024. doi:10.1038/s42256-024-00861-3. URL <https://doi.org/10.1038/s42256-024-00861-3>.
- [25] S. Abeyruwan, A. Bewley, N. M. Boffi, K. M. Choromanski, D. B. D’Ambrosio, D. Jain, P. R. Sanketi, A. Shankar, V. Sindhwani, S. Singh, et al. Agile catching with whole-body mpc and blackbox policy learning. In *Learning for Dynamics and Control Conference*, pages 851–863. PMLR, 2023.

- [26] A. Ghadirzadeh, A. Maki, D. Kragic, and M. Björkman. Deep predictive policy training using reinforcement learning. In *2017 IEEE/RSJ International Conference on Intelligent Robots and Systems (IROS)*, pages 2351–2358. IEEE, 2017.
- [27] C. Wang, S. Wang, B. Romero, F. Veiga, and E. Adelson. Swingbot: Learning physical features from in-hand tactile exploration for dynamic swing-up manipulation. In *2020 IEEE/RSJ International Conference on Intelligent Robots and Systems (IROS)*, pages 5633–5640. IEEE, 2020.
- [28] Z. Lončarević, R. Pahič, M. Simonič, A. Ude, and A. Gams. Reduction of trajectory encoding data using a deep autoencoder network: robotic throwing. In *Advances in Service and Industrial Robotics: Proceedings of the 28th International Conference on Robotics in Alpe-Adria-Danube Region (RAAD 2019) 28*, pages 86–94. Springer, 2020.
- [29] C. Florensa, D. Held, X. Geng, and P. Abbeel. Automatic goal generation for reinforcement learning agents. In *International conference on machine learning*, pages 1515–1528. PMLR, 2018.
- [30] M. Plappert, M. Andrychowicz, A. Ray, B. McGrew, B. Baker, G. Powell, J. Schneider, J. Tobin, M. Chociej, P. Welinder, V. Kumar, and W. Zaremba. Multi-goal reinforcement learning: Challenging robotics environments and request for research. *arXiv preprint arXiv:1802.09464*, 2018.
- [31] H. Kasaei and M. Kasaei. Throwing objects into a moving basket while avoiding obstacles. In *2023 IEEE International Conference on Robotics and Automation (ICRA)*, pages 3051–3057. IEEE, 2023.
- [32] K. Fang, P. Yin, A. Nair, and S. Levine. Planning to practice: Efficient online fine-tuning by composing goals in latent space. In *2022 IEEE/RSJ International Conference on Intelligent Robots and Systems (IROS)*, pages 4076–4083. IEEE, 2022.
- [33] S. Nasiriany, V. Pong, S. Lin, and S. Levine. Planning with goal-conditioned policies. *Advances in neural information processing systems*, 32, 2019.
- [34] M. Liu, M. Zhu, and W. Zhang. Goal-conditioned reinforcement learning: Problems and solutions. In L. D. Raedt, editor, *Proceedings of the Thirty-First International Joint Conference on Artificial Intelligence, IJCAI-22*, pages 5502–5511. International Joint Conferences on Artificial Intelligence Organization, 7 2022. doi:10.24963/ijcai.2022/770. URL <https://doi.org/10.24963/ijcai.2022/770>. Survey Track.
- [35] E. Chane-Sane, C. Schmid, and I. Laptev. Goal-conditioned reinforcement learning with imagined subgoals. In *International conference on machine learning*, pages 1430–1440. PMLR, 2021.
- [36] Y. Liu, A. Gupta, P. Abbeel, and S. Levine. Imitation from observation: Learning to imitate behaviors from raw video via context translation. *IEEE International Conference on Robotics and Automation*, 2017. doi:10.1109/ICRA.2018.8462901.
- [37] J. Ho and S. Ermon. Generative adversarial imitation learning. *Neurips*, 2016.
- [38] M. Reuss, M. Li, X. Jia, and R. Lioutikov. Goal-conditioned imitation learning using score-based diffusion policies. *Robotics: Science and Systems*, 2023. doi:10.48550/arXiv.2304.02532.
- [39] A. Jain and V. Unhelkar. Go-dice: Goal-conditioned option-aware offline imitation learning via stationary distribution correction estimation. In *Proceedings of the AAAI conference on artificial intelligence*, volume 38, pages 12763–12772, 2024.

- [40] D. Ghosh, A. Gupta, A. Reddy, J. Fu, C. Devin, B. Eysenbach, and S. Levine. Learning to reach goals via iterated supervised learning. *Iclr*, 2021.
- [41] S. Lee, Y. Wang, H. Etukuru, H. J. Kim, N. M. M. Shafiullah, and L. Pinto. Behavior generation with latent actions. In *Forty-first International Conference on Machine Learning, ICML 2024, Vienna, Austria, July 21-27, 2024*. OpenReview.net, 2024. URL <https://openreview.net/forum?id=hoVwecMqV5>.
- [42] S. Haldar, J. Pari, A. Rai, and L. Pinto. Teach a robot to fish: Versatile imitation from one minute of demonstrations. *Robotics: Science and Systems*, 2023.
- [43] J. Carvalho, D. Koert, M. Daniv, and J. Peters. Residual robot learning for object-centric probabilistic movement primitives. *arXiv preprint arXiv:2203.03918*, 2022.
- [44] T. Silver, K. Allen, J. Tenenbaum, and L. Kaelbling. Residual policy learning. *arXiv preprint arXiv:1812.06298*, 2018.
- [45] L. Ankile, A. Simeonov, I. Shenfeld, M. Torne, and P. Agrawal. From imitation to refinement - residual rl for precise assembly. *arXiv preprint arXiv: 2407.16677*, 2024.
- [46] Y. Seo, J. Uruç, and S. James. Continuous control with coarse-to-fine reinforcement learning. *Conference on Robot Learning*, 2024. doi:10.48550/arXiv.2407.07787.
- [47] L. X. Shi, Z. Hu, T. Z. Zhao, A. Sharma, K. Pertsch, J. Luo, S. Levine, and C. Finn. Yell at your robot: Improving on-the-fly from language corrections. *Robotics - Science and Systems*, 2024.
- [48] A. Ajay, J. Wu, N. Fazeli, M. Bauza, L. P. Kaelbling, J. B. Tenenbaum, and A. Rodriguez. Augmenting physical simulators with stochastic neural networks: Case study of planar pushing and bouncing. In *2018 IEEE/RSJ International Conference on Intelligent Robots and Systems (IROS)*, pages 3066–3073. IEEE, 2018.
- [49] A. Kloss, S. Schaal, and J. Bohg. Combining learned and analytical models for predicting action effects. *arXiv preprint arXiv:1710.04102*, 11, 2017.

A Method Details

A.1 Formulations

The perceptron P is set to account for the inaccuracies of perception results. The assumption we made in the main text all aim to make it consistent with how human estimate error feedback, and they can be explained with example task *Basketball Shot* as follows:

- **Each dimension is independently estimated:** By watching their last throw attempt, the player might judge that the ball lands about 15 cm to the left and 30 cm shorter. Each of these 2 measurements might contain errors, but they can hardly affect each other. This is based on the daily experience that human can easily judge whose x is larger among 2 points with clearly defined axis, even if their y are different.
- **Monotonicity:** If the estimated result is that the ball lands 15 cm to the left, this number might not be accurate, but this shot must land closer to the hoop than another shot that is estimated to land 20 cm to the left.
- **Zero limit:** $\lim_{e \rightarrow 0} ||e - P(e)|| = 0$. Estimation of shorter distance contains lower absolute errors. (e.g. 80 cm might be inaccurately estimated to be 100 cm with 20 cm errors, but 8 cm can never be estimated to be 28 cm)

Algorithm 1 Adaptive Diffusion Action Planning (ADAP)

Inputs: Environment Env , estimated goal $\tilde{\mathbf{g}}$, rough error perceptron P , prior demonstration dataset $D_{\text{prior}} = \{\mathbf{A}_i\}$, goal-conditioned action planner $\pi : \tilde{\mathbf{r}} \rightarrow \mathbf{A}$, Bayesian-optimization based mapping M and corresponding dataset D_M .

Stage 1: Motion Pattern Learning

- 1: Rollout all action plans \mathbf{A}_i in D_{prior} to construct dataset D_e :

$$D_e = \{(\mathbf{A}_i, \tilde{\mathbf{r}}_i) \mid \tilde{\mathbf{r}}_i = P(\text{rollout}(\mathbf{A}_i) - \mathbf{g}_0), \mathbf{A}_i \in D_{\text{prior}}, \mathbf{g}_0 = \mathbf{0}\}$$

- 2: Train goal-conditioned diffusion planner π using D_e .

Stage 2: Iterative Rollout & Adaption

- 3: Initialize dataset D_M with identity mapping:

$$D_M = \{(\mathbf{c}_i, \tilde{\mathbf{g}}_i) \mid \mathbf{c}_i = \tilde{\mathbf{g}}_i = \tilde{\mathbf{r}}_i, (\mathbf{A}_i, \tilde{\mathbf{r}}_i) \in D_e\}$$

- 4: **repeat**

- 5: Get condition $\mathbf{c}^{\text{new}} = M(\tilde{\mathbf{g}})$ and generate new action plan $\mathbf{A}^{\text{new}} = \pi(\mathbf{c}^{\text{new}})$.

- 6: Rollout \mathbf{A}^{new} to obtain error $\tilde{\mathbf{e}}^{\text{new}} = \tilde{\mathbf{e}}_{\mathbf{g}}(\mathbf{c}^{\text{new}})$ by Equation 5.

- 7: Augment D_M to update the mapping M :

$$D_M \leftarrow D_M \cup \{(\mathbf{c}^{\text{new}}, \tilde{\mathbf{g}} + \tilde{\mathbf{e}}^{\text{new}})\}$$

- 8: **until** $\tilde{\mathbf{e}}^{\text{new}} \approx \mathbf{0}$

- 9: **Output:** Final successful action plan $\mathbf{A}_f = \mathbf{A}^{\text{new}}$
-

From these assumptions we see that P is allowed to only provide really rough estimations. Throughout all our experiments in real-world, this P is implemented by raw human eye, which means that we just provide a distance estimation with a simple glance of a specific rollout without measuring it carefully with tools like rulers. Specifically, we only provide 1 cm, 2 cm, 3 cm, 4 cm and multiplies of 5 cm as choices of each dimension of the estimated error $\tilde{\mathbf{e}}$, such accuracy is in accordance with human requirements for learning such tasks.

A.2 Techniques

The **Timeline Shifting Augmentation** technique involves the following operation on an action plan $\mathbf{A} = \{\mathbf{a}_t \mid t \in [H]\}$, as presented in Algorithm 2. This process randomly shift the action plan along the timeline for a random number of shift steps, and pad the remaining blanks by repeating the nearest frame-action. The core idea is that the motion always happen in the central part of the timeline, and the rollout results do not rely on the starting frame of motion. Thus by augmenting the training set by Timeline Shifting, the planner π tends not to memorize the frame action of specific timesteps, but to focus more on learning the motion pattern that is independent of the timeline.

Algorithm 2 Timeline Shifting Augmentation

- 1: shift_steps = random_int(1, shift_steps_upperbound)

- 2: **if** random_bool() **then**

$$\mathbf{A}[\text{shift_steps} :] = \mathbf{A}[: -\text{shift_steps}]$$

$$\mathbf{A}[: \text{shift_steps}] = \mathbf{A}[0]$$

- 3: **else**

$$\mathbf{A}[: -\text{shift_steps}] = \mathbf{A}[\text{shift_steps} :]$$

$$\mathbf{A}[-\text{shift_steps} :] = \mathbf{A}[-1]$$

- 4: **end if**
-

B Detailed Task Setups in Lab

Here we list the detailed descriptions of the three real-world tasks introduced in Section 2. Please refer to Figure 1 for better understanding of the task process. Besides, we provide close-ups of the hardware involved in Figure 5.



Figure 5: Hardware involved in real-world tasks:

Left: Hardware for *Basketball Shot* (V1) and its 2 modified versions V2 and V3. The original version V1 uses the hoop (diameter = 9.0 cm, white spoon to throw the bigger ball (diameter = 6.0 cm) into the hoop; V2 changes to the shorter blue spoon based on V1; V3 changes to the smaller lighter ball and replace the hoop by a smaller cup, based on V2.

Right Upper: Hardware for *Curling*.

Right Lower: Hardware for *Fishing Rod Swinging*. We borrow a curling stone from the last task to make use of the iron ball inside. The small magnet is just enough to catch the iron ball in very close distance (about 0.5 cm).

B.1 Basketball Shot

Scene: In this task, we set a Franka-Emika robot with a spoon-shaped end effector attached to its flange to throw the toy basketball forward. The initial posture of the robot is assumed to be fixed so that the ball can be placed steadily in a fixed proper position before launching. The smooth contact face of the spoon-shaped end effector allows the ball to detach naturally from it through smooth acceleration changes, just like how real basketballs detach from human’s hands. The goal is to let the ball fall into the hoop that locates arbitrarily in an effective range on the table. Note that the diameter of the ball is 6 cm and the hoop is only 9 cm, only 1.5 times larger than the ball, while this proportion for real basketball is 1.8, which means ours requires higher accuracy.

Success Metric: The ball precisely penetrates the hoop.

Feedback Form: For failed trials, the feedback is the relative 2D coordinate of the ball’s landing point on the hoop plane with respect to the hoop center, which is estimated by raw human eye.

Priors: The prior demonstration set D_{prior} is generated from a mirror environment built in the Isaac-Gym simulator. We adopt a B-spline representation to reduce the dimensionality of action plans, and rollout a larger number of random trials then finally filter out about 10 plans to be proposals for the prior demonstration dataset.

B.2 Curling

Scene: In this task, we set a Franka-Emika robot with a var-shaped end effector attached to its flange to push a toy curling stone sideways. The initial posture of the robot is fixed, and the curling stone to be pushed (blue) is always manually placed at the middle of the pushing part, before any rollouts. The goal is to push out the blue stone so that it slides until collides slightly with the red stone (which is placed arbitrarily in an effective range on the table) then stops. The diameters of the stones are only 3 cm.

Success Metric: The blue stone slightly collides with the red stone then stops. The final distance between them is less than the diameter.

Feedback Form: For failed trials, the feedback is the relative 2D coordinate of the blue stone’s landing point on the table with respected to the red stone, which is estimated by raw human eye. If a collision happens but the stones moved far away afterwards, we still estimate a rough landing point in imagination, assuming that the collision does not happen.

Priors: The demonstrations for this task were collected using a Quest VR controller for tele-operation, and we apply a post-processing by motion planning based on the collected demonstration data, to eliminate the random movement along the z-axis induced by inaccuracies of the tele-operation hardware and the robot arm itself.

B.3 Fishing Rod Swinging

Scene: In this task, we employ a Franka-Emika robotic arm, equipped with a rod attachment, at the end of which a string is suspended. A small metal weight is affixed to the lower end of the string. Beneath the apparatus, a small magnet is positioned. The objective is to maneuver the rod in such a manner that the metal weight swings toward the magnet, landing directly above it. Once in position, the magnetic attraction between the metal weight and the magnet ensures successful docking. Due to the small size of the magnet, successful docking can only occur when the metal weight approaches directly from above.

Success Metric: Success is achieved only when the metal weight lands directly on top of the magnet and becomes magnetically attached. This requires error less than about 1 cm. Any other landing position, even if close to the magnet, is considered a failure.

Feedback Form: For failed trials, the feedback is the relative 2D coordinate of the metal weight’s landing point with respect to the magnet’s position, which is estimated by raw human eye. This provides spatial information about how far and in which direction the landing attempt missed the target.

Priors: The demonstrations for this task were collected using a Quest VR controller for tele-operation, and we limit the rotational degrees during data collection due to the low quality of the collected data on such dimensions.

C Simulator Experiment Details

C.1 Simulator Task Settings

We run all baselines on the *Basketball Shot* task environment built in IsaacGym simulator that serves as a twin-copy of the real-world one. (Length and size of all hardware remain consistent.) This allows us to repeat the experiments efficiently on large number of goals. The 100 goals are set to be the same for all baselines, which spread evenly on a 0.4 m * 0.5 m area on the table. We do not set a concrete hoop but instead directly measure the distance between the landing location and the goal, where a <3 cm result is judged be a successful hit. All baselines share the same prior set D_{prior} (except slightly modified for the last one), and we set the same 100 goals that spread evenly within the reachable range, and run 10 rounds of adaption.

C.2 Details of Some Baselines

Interpolation of Nearest Neighbors: In this baseline, the diffusion based conditional action planner π of ADAP is replaced by the following one, denoted as π_{INN} : Given condition \mathbf{c} , we find the nearest 3 neighbors in D_e , represented by $(\mathbf{A}_i, \mathbf{r}_i)$, $1 \leq i \leq 3$. We solve for the weights w_i such that $\sum_{i=1}^3 w_i \cdot \mathbf{r}_i = \mathbf{c}$, and then directly compute the weighted sum by $\mathbf{A}_p = \sum_{i=1}^3 w_i \cdot \mathbf{A}_i = \pi_{\text{INN}}(\mathbf{c})$ as the output of this new planner π_{INN} .

Interpolation of Nearest Neighbors Aligned: The action plans in dataset D_e involve motions starting from different timesteps, to stay consistent with real-world scenes where demonstration may come from noisy sources. In this baseline we modify D_e to align the periods of motions (inside the action plans) together, so that linear interpolation achieves best performance.

C.3 Results Analysis

From the result statistics shown in Figure 4 we can see that: *Timeline Shifting Augmentation* increase the performance a lot by letting π focus on learning the motion patten while avoiding overfitting to the small dataset; *Data Forgetting* provides small increment on the converged success rate by dropping the possibly dirty data that limits the condition adaption quality. *Interpolation of Nearest Neighbors* can reach a certain performance only if the prior demonstrations are carefully aligned along the timeline, but this condition are hardly be satisfied when demonstrations are coming from other real-world sources, and it fails completely when this alignment is not satisfied.

D Hyperparameters

Here we list the hyperparameters involved in our experiments (both for real-world and simulator). Most hyperparameters remain unchanged with respect to those of Chi et al. [19] (U-Net) except the learning rate.

Model Component	Hyperparameter	Value
Bayesian Optimizer Kernel	Constant kernel amplitude	1.0
	RBF kernel length scale	1.0
Gaussian Process Regressor	Optimizer restart count	5
	Observation noise level α	1×10^{-6}
Noise Scheduler	Number of training timesteps	100
	Beta start	0.0001
	Beta end	0.02
	Beta schedule	squaredcos_cap_v2
	Variance type	fixed_small
Training Configuration	Prediction type	epsilon
	Batch size	256
	Horizon for <i>Basketball Shot</i>	140
	Horizon for <i>Curling</i> and <i>Fishing Rod Swinging</i>	200
Optimizer	Type	AdamW
	Learning rate	5.0×10^{-4}
	Betas	[0.95, 0.999]
	Epsilon	1.0×10^{-8}
	Weight decay	1.0×10^{-6}
EMA Configuration	LR scheduler	constant
	Update after step	0
	Inverse gamma	1.0
	Power	0.75
Training Schedule	Max value	0.9999
	Number of epochs	3000
	LR warmup steps	500
	Gradient accumulation steps	1

Table 3: Hyperparameters